LiNbO3 integrated optic devices with an UV-curable polymer buffer layer

Woon-Jo Jeong*, seong-Ku Kim**, Gye-Choon Park***, Jin Lee****

*Dept. of Information & Telecommunication, Hanlyo University
**Dept. of Electrical Engineering, University of California at Los Angeles
***Dept. of Electrical Engineering, Mokpo National University
****Dept. of Control & Instrumentation Engineering, Mokpo National University

Abstract

A new lithium niobate optical modulator with a polymer buffer layer on *Ni* in-diffused optical waveguide is proposed for the fist time, successfully fabricated and examined at a wavelength of *1.3 mm* . By determining the diffusion parameters of *Ni* in-diffused waveguide to achieve more desirable mode size which is well matched to the mode in the fiber, the detailed results on the achievement of high optical throughput are reported. In addition, the usefulness of polymer buffer layer which can be applicable to a buffer layer in *Ni* in-diffused waveguide devices is demonstrated. Several sets of channel waveguides fabricated on *Z*-cut lithium niobate by *Ni* in-diffusion were obtained and on which coplanar traveling-wave type electrodes with a polymer-employed buffer layer were developed by a conventional fabrication method for characterizing of electro-optical performances of the proposed device. The experimental results show that the measured half-wave voltage is of *~10 V* and the total measured fiber-to-fiber insertion loss is of *~6.4 dB* for a *40 mm* long at a wavelength of *=1.3 mm*, respectively. From the experimental results, it is confirmed that the polymer-employed buffer layer in *LiNbO3* optical modulator can be a substitute material instead of silicon oxide layer which is usually processed at a high temperature of over *300* ℃. Moreover, the fabrication tolerances by using polymer materials in *LiNbO3* optical modulators are much less strict in comparison to the case of dielectric buffer layer.

Keywords: Nickel in-diffusion. Optical Modulator, Polymer Buffer Layer, Traveling-wave type Coplanar Waveguide Electrode, Mode Size

1. Introduction

The two mainly used techniques for the fabrication of $LiNbO_3$ optical waveguides are Ti in-diffusion and proton exchange [1, 2]. Ti in-diffusion is a high temperature process that increases both ordinary and extraordinary indices ($\triangle n_o$ and $\triangle n_e$), and gives waveguides both the ordinary and extraordinary polarizations in $LiNbO_3$ [3]. Proton exchange is a relatively low-temperature process that provides waveguides with supporting only the extraordinary polarizations ($\triangle n_o<0$ and $\triangle n_e>0$). For some applications, a singly polarized waveguide can be desirable for better device performances so that the interaction between the *TM* and *TE* waves can be avoided. Recently, not only *TE* but also *TM* and both *TE/TM* polarized waveguides have been demonstrated by *Ni* in-diffusion, which can be obtained by varying the fabrication conditions of *Ni* in-diffusion [4]. Furthermore, one of important advantages in *Ni* in-diffused waveguides is relatively low-diffusion process in compare with *Ti* in-diffusion, so that there is no out-diffusion guiding layer by Li_2O and no changing electro-optic coefficient [5]. In addition, some similar performances in the effective indices and the losses of the *Ni* in-diffused waveguides as compared to that of *Ti*

in-diffused waveguide have been obtained [3-5].

However, most of common $LiNbO_3$ modulators have been employed a buffer layer of SiO_2, because a metallic layer, such as gold-electrodes, induces high propagation loss in guided optical fields. The process of SiO_2 layer requires a high temperature of over *300* ℃ to form a reasonable quality of deposited SiO_2 layer on the top of $LiNbO_3$ waveguides, but in case of *Ni* in-diffused waveguides such a high temperature may induce un-expected index changes in *Ni* in-diffused waveguide because of rapid diffusion of *Ni* metal source into $LiNbO_3$ substrate [1, 6]. On the other hand, a fabrication process with a polymer material to build the similar buffer layer on $LiNbO_3$ waveguides can be significantly simple as compared to the traditional process of $LiNbO_3$ waveguides due to the low temperature process and easy control of a polymer material. This polymer is originally used for making polymer waveguides in the integrated optic areas as seen in [9].

From the earlier reported papers [1-8], *Ni* in-diffusion method can be a good alternative in the $LiNbO_3$ integrated optic devices, but the optimum fabrication condition of the *Ni* in-diffused waveguides for the fiber-pigtail has not been established at this point. Furthermore, there are several applications of *Ni* waveguides such as Mach-Zehnder interferometric modulators, directional couplers and splitters, but any competitive result against *Ti*: $LiNbO_3$ waveguides has not been reported till now.

Therefore, in this work, further investigations into *Ni* in-diffused waveguides regarding to the fabrication condition of optimum mode in *Ni* in-diffused waveguides and its optical confinement including the polymer buffer layer effect on the driving voltage have been carried out under several diffusion condition at a wavelength of *1.3 mm*.

2. Fabrication and measurement

Several sets of waveguides were fabricated by diffusing *Ni* film evaporated onto a *LiNbO3* substrate in a tube furnace at a temperature of *900* ℃ for diffusion time ranging from 1 to 3 *h*. All channel waveguides before diffusion have a width of *8 mm*, and *Ni* thickness of *300* Å. The *Z*-cut $LiNbO_3$ wafers were used for the fabrication of waveguide. After diffusing, a UV-curable epoxy (*UV-15*, Masterbond Co.) layer was spun on diffused waveguides to give a buffer layer between optical waveguides and metal electrodes. The gold electrodes of *1.5 mm* thickness were formed by electroplating and diced to each device. The device end-faces were cut without an angle to the waveguides and then polished to an optical finish. A good optical end face and a sharp edge were obtained at both the input and output optical facets of the device to ensure good fiber-to-waveguide coupling. The schematic diagram for the fabrication process is shown in Figure 1. The optical measurement was performed at *1.3mm* wavelength. A polarization maintaining fiber for the input pigtail was utilized to launch the optical power and was attached to the waveguides by using an *UV*-curable Index matching oil, while the output fiber was a standard single-mode fiber. The sample size used for coupling with fibers was all about *45 mm3 mml mm*. The output of a *1.3 mm* source is

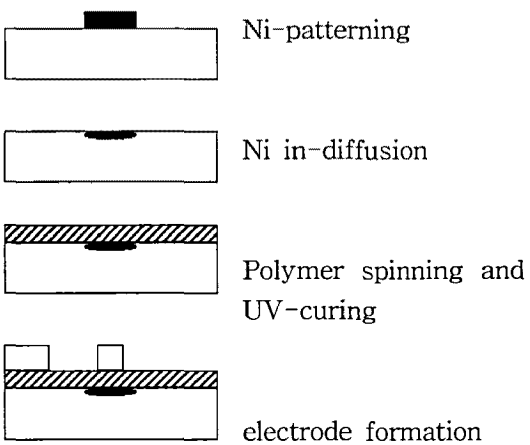

Fig. 1. Fabrication process of an *Ni:LiNbO3* integrated optic device with a polymer buffer layer.

used to excite the devices through PMF and SMF. To investigate the waveguide performance, first a *He-Ne* laser with a wavelength of *0.6328 mm* was utilized to identify the optical power and which is coupled with a laser source of *1.3 mm* wavelength (Lightwave Electronics Co.) via 2x2 coupler. The images from the waveguides were projected to a CCD camera used to view the optical mode image. Once the image was focused on it with some distance, the near field pattern of the waveguide could be captured and then compared with that of a standard single mode fiber to evaluate the mode characteristics. A polarization rotator inserted between waveguide and photo-detector also was used to observe the polarization states from the waveguide output.

3. Results and discussion

In order to investigate the optical intensity distribution of the *Ni* in-diffused waveguide output power that is required to get a mode match to a single mode fiber, Near-field patterns of a series of fabricated channel waveguides were observed. Figure 2 shows the variation of mode sizes of fabricated *Ni* in-diffused waveguides with several diffusion time along the width and depth direction of the channel waveguide, respectively. The mode diameters in width and depth directions were evaluated at the 1/e point of each near field pattern for comparison.

From the figure 2, it is found that the mode sizes in depth and width of waveguides were slightly dependent on the diffusion time for the fundamental *TM* mode. As diffusion time increases, the mode size in depth increases rapidly. On the other hand, the mode size in width was not changed too much along the diffusion time. However, making the diffusion time shorter, the optical confinement of the guided mode becomes much stronger. The sample at a diffusion time of *1 h* has mode size of *4.54 mm* in depth and *7.52 mm* in width, that is, the shorter diffusion time can make the mode size a short. On the other hand, in case of diffusion time of *3 h*, the mode size shows *7.68 mm* in depth and *8.86 mm* in width.

It has been considered that the fiber-to-fiber insertion loss is also strongly depend on the mode size of the fabricated channel waveguides that is related to the fabrication condition of making well confined optical waveguides. In order to prepare the more strongly confined optical waveguide, first the diffusion depth must be short, and second the index change in waveguides must be increased : the former corresponds to making the diffusion time a short, the latter corresponds to the amount of diffusion source used before *Ni* diffusion which must be increased. If the *Ni* thickness before diffusion is applied upto *400* Å, multimode waveguides will usually be obtained at the *1.3 mm* wavelength. It is also reported that the critical thickness of the *Ni* film with a waveguide width of *8 mm* is almost *300* Å [4], so that in this work, the diffusion source, *Ni* thickness, remains a constant of *300* Å. By varying the diffusion time instead, the appropriate mode size comparable to that of a standard single mode fiber was investigated.

As seen from [12], in case of the well confined optical waveguides, a shorter diffusion time can give a lower driving voltage (*20 %* lower than a longer one), but a total insertion loss might be increased (*50 %*) due to the mode mismatch between waveguides and attached fibers. This means that the coupling loss will be increased too much dramatically. Therefore, there is a trade-off between the two factors, well confined waveguide and fiber-coupling. It is considered that the best diffusion time at this point which has more desirable mode size comparable to a single mode fiber was turned out to be a diffusion time of *3 h*. In other words, among the examined conditions, even though waveguides fabricated by diffusion time of *1 h* with a diffusion temperature of *900 °C* looks like having an excellent optical confinement, the waveguides fabricated under *900 °C* for *3 h* has more appropriate mode sizes in depth of *8.86 mm* and

width of *7.68 mm* to that of a single mode optical fiber which usually has *8~10 mm* of core size. Practically, the mode size and shape are important characteristics of practical devices, and they determine the minimum interference loss between the waveguide and pigtailed single mode fiber [7, 8]. Therefore, from the above result, it is confirmed that the waveguides fabricated with *300* Å of *Ni* thickness with a diffusion time of *3 h* at a diffusion temperature of *900* °*C* exhibited mode size most compatible with that of the fiber.

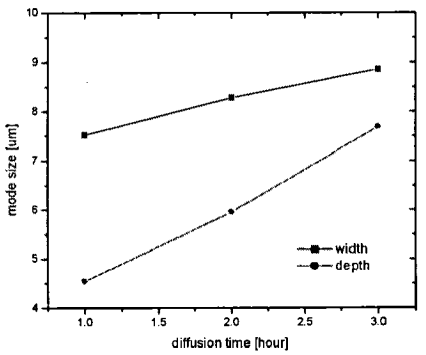

Fig. 2. Optical output distribution of Ni in-diffused channel waveguides in depth and width for the fundamental TM mode at a wavelength of 1.3 mm under a diffusion temperature of 900 ℃.

Optical loss is a main factor of primary concern in practical applications with integrated optic devices [13, 14]. In general, the pigtailed optic devices show three kinds of optical losses : (a) reflection loss (Fresnel reflection), which is mainly due to the difference in the refractive indices between the fiber pigtail and the waveguide. This factor can be reduced enough to be as low as *~0.1 dB* by using index matching fluid ; (b) propagation loss, which accounts for the scattering and absorption of light inside the device that will be demonstrated at the bottom of this chapter ; and (c) coupling loss, which includes the loss due to mode-field mismatch between the fiber and the waveguide, and the scattering loss at the fiber-waveguide interface. The factor (c) was mainly focused to look for an optimum mode size of *Ni* in-diffused waveguide that is well matched to that of the fiber and also gives the waveguides an optimum fabrication condition, then the contributions of propagation and coupling loss to the total insertion loss were determined.

In the case of the diffusion condition of *900* ℃ for diffusion time of *3 h*, the near field optical contour profile and the mode profile in depth and width direction are shown in Figure 3. It is also believed that it has excellent optical confinement and less substrate radiation. The waveguide mode profile in the depth direction is a little asymmetric as expected and the mode shape in width was essentially Gaussian mode. Also the mode profile of the fiber was measured and mode diameter at the 1/e intensity was turned out to be *7.58 mm*. In the case of *TE* polarization in the fabricated waveguides, the mode size was much wider than *TM* polarization and the 1/e points for mode size measurements were not considered because the proposed device has only used the one-direction of *TM* polarization. Therefore, From this evaluation, *Ni* in-diffused channel waveguides fabricated with *300* Å of metal thickness for diffusion time of *3 h* exhibited mode size was most compatible with that of the fiber in this work.

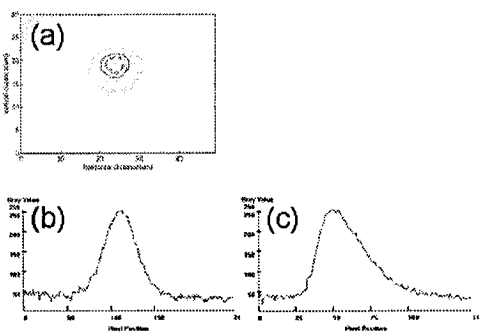

Fig. 3. Optical contour profile (a) and mode size in width (b) and depth (c) of the fundamental TM mode of the Ni in-diffused channel waveguide at a wavelength of 1.3 mm. The fabrication condition was diffusion time of 3 h, temperature of 900 ℃, and Ni thickness of 300 Å.

The expected coupling efficiency can be evaluated by computing the overlap integral between the fiber and the measured modes for *Ni* in-diffused channel waveguide. A power coupling coefficient can be written as [15]

$$k = 0.93\left[\frac{4}{(w_x/a + a/w_x)(w_y/a + a/W_y)}\right] \quad (1)$$

Where a is the fiber mode diameter at 1/e optical intensity, and wx is the measured 1/e intensity full width and wy is full depth, respectively. More conveniently [16], to investigate the dimensional dependence of the expected coupling loss, the power coupling coefficient can be written as

$$k = 0.93\left[\frac{4(w/a)^2}{(w/a)^2 + \varepsilon)((w/a)^2 + 1/\varepsilon)}\right] \quad (2)$$

Where w is the geometric mean, $w=(w_x\ w_y)$, and is the ratio of the waveguide mode width to depth $= w_x / w_y$. It is shown that the calculated coupling loss per interface is a function of a dimensional mismatch between the fiber and waveguide modes versus the ratio of the waveguide mean diameter to the fiber diameter. The measured 1/e intensity full width wx and depth wy for the *Ni* waveguide with diffusion time of *3 h* are *8.86 mm* and *7.68 mm* for *TM* polarization, respectively. The ratio ε was about 1.53 that approaches unity for waveguides near cutoff. Equation (2) also indicates that the optimum coupling can be achieved for $w=a$ regardless of the mode eccentricity between wx and wy. At this condition, a constant factor of coupling loss can be derived as *~0.315 dB* which is conservative through a fiber-to-waveguide pigtail, therefore the total expected coupling loss per interface is the sum of the value given by equation (2) [15,16,17]. According to the relationship between w/a and coupling loss in equation (2), the coupling loss is less sensitive to non-unity eccentricity. For example, a *15* percent error deviated from optimum condition $\varepsilon = 1$ can causes an increase of the coupling loss by ~0.05 dB for our case of $w/a=1$. The fabrication condition of *Ni* thickness of *300* Å and diffusion time of *3 h* gives the aspect ratio, of *1.53* which contributes *0.085 dB* per interface to the coupling loss, thus according to the equation (2), the total expected coupling loss will *be 0.526 dB* per interface.

In order to determine the relative contribution of coupling and propagation loss to the total insertion loss, the devices were aligned with fibers, a PMF for input end-face and a SMF for output end-face of a channel waveguide, and a perfect fiber-waveguide alignment was assumed. The coupling loss was evaluated as following simple method; (1) at the output end-face, the projected output power was expanded by objective lens and then measured the intensity of the optical power by a photo-detector. (2) After that, a SMF was attached to the output channel waveguide with an index matching oil and the output power was measured as a total insertion loss. From the result in difference value between the measured loss for *TM* polarization, the coupling loss per interface can be calculated and this value includes a residual Fresnel loss per face. The coupling loss of *~0.43 dB* and propagation loss of *1.39 dB/cm* have been achieved. The total measured fiber-to-waveguide-to-fiber insertion loss for *4.5 cm* long waveguide was as low as *~7.12 dB*. It is noticed that the estimated value of the coupling loss of *0.43 dB* was lower than the calculated one of *0.526 dB*, so that the waveguide mode in depth is probably less mismatched to that of the fiber than the introduced Hermite-Gaussian profile.

For evaluating the thickness effect of polymer buffer layer on the driving voltage of the fabricated devices, a simple closed-form solution was used to calculate the optical-electrical field overlap as a function of the thickness of the polymer buffer layer [8, 11, 18]. An electrode structure of the device to be considered is a traveling-wave coplanar waveguide type electrode which is usually incorporated to high speed modulators. The relative permittivity tensor of

lithium niobate substrate displays a strong anisotropy $x=43$ and $y=28$. On the other hand, the buffer layer which is commonly used for a optical polymer device is *UV-15* that has a very low viscosity and is an UV-curable polymer. According to the experimental data [19], it has been shown that the dielectric constant is $\varepsilon_x = \varepsilon_y = 3.21$ at a frequency of *1 GHz*. On *Z*-cut $LiNbO_3$, the horizontal and vertical electric field produces an optical phase shift through the r_{33}, r_{21}, and r_{33} electro-optic coefficient. Thus the field distribution of the electric field as a function of the buffer layer thickness of waveguide is of importance because of depending on the device performance. First, in order to evaluate the overlap integral of optical and electrical field profile quantitatively, the electric field distributions a function of x and y position is required. After deriving the overlap integral of the optical and electric fields, the driving voltage which is required to turn the modulator from full on to full off can be calculated. The field distribution $E(x,y)$ of the z-directed electric field [10,11,18] for a symmetric coplanar waveguide type electrode can be derived numerically. On the other hand, the transverse field profile $E_{op}(x,y)$ of the optical waveguide can be expressed by a Hermite-gaussian function. And also an overlap integral of the optical field profile with the electric field profile is quantitatively evaluated

$$\Gamma = \frac{V_0}{S} \frac{\int_0^{\infty}\int_b^a E_{op}(x,y)^2 E_{el}(x,y)\,dxdy}{\int_0^{\infty}\int_b^a E_{op}(x,y)^2\,dxdy} \qquad (3)$$

The driving voltage V can be expressed as

$$V_{\pi} = \lambda \frac{S}{2(n^3 r_{33} L\Gamma)} \qquad (4)$$

Where is the optical wavelength, n is the optical refractive index, L is the length of the electrode, r_{33} is the electro-optic coefficient that produces a phase change for light polarized in z-direction for a z-directed applied electric field, and is the overlap integral. Figure 4 shows the calculated driving voltage as a function of buffer layer thickness. As shown in this figure, as the polymer buffer layer increases, the driving voltage becomes higher because of a small value of the polymers relative electrical permittivity [20] which layer attenuates the magnitude of electric field in waveguides efficiently more than that of SiO_2 buffer layer. As a matter of fact, it would obviously be desirable to have a material with a higher dielectric constant than *UV-15*. As an example of the calculated results, a buffer layer of *1 mm* with silicon oxide gives a driving voltage of *5.8V* ; on the contrary, a polymer buffer layer of *1 mm* gives a driving voltage of *9.5 V* which value is over *59* percent higher than that of silicon oxide buffer layer according to the same calculation with the relativity permittivity of *4.0* for silicon oxide [21]. In order to realize an acceptable performance with a driving voltage, the buffer layer thickness should be determined by ~ 0.5 *mm* to keep the driving voltage less than *7 V*.

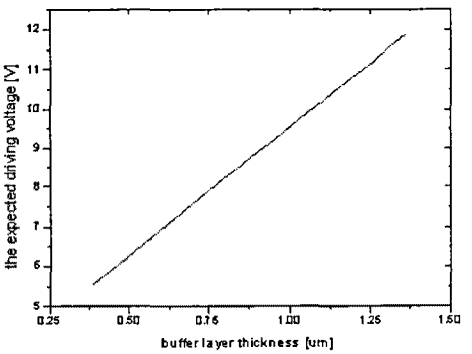

Fig.4. Calculated increase in driving voltage as a function of UV-15 polymer buffer layer thickness with a interaction region L=20 mm.

Fig.5 (a) shows the modulation output of the fabricated Ni in-diffused lithium niobate modulator operating at a wavelength *1.3mm* wavelength that is corresponding to the diffusion

condition of *900 °C* for *3 h*. The thickness of polymer buffer layer and electrode thickness was *0.75 mm* and *1.5 mm*, respectively. The measured half-wave voltage was about *9.89 V*. As indicated in figure 4(a), the expected driving voltage (half-wave voltage) was less than *8 V*, but there was a deviation of driving voltage by *2 V*. This measured value was much worse than the simulation result as described above. A possible reason showing a worse driving voltage would be the fabrication error which could be caused by a misalignment between waveguide and electrodes. Another reason is that the simulation method may lead to inaccurate result at this point. The measured electro-optical modulation shows that the extinction ratio is high of *17.5 dB* enough for practical applications. The picture in Fig.5 (b) shows one of devices aligned with fibers in both sides of waveguide.

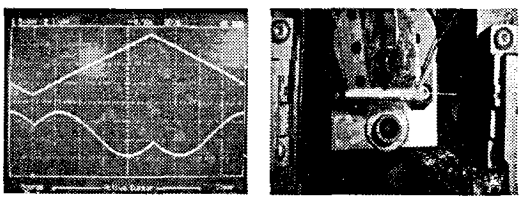

Fig.5. (a) The modulation performance of a Ni in-diffused modulator at a 1.3 mm wavelength under diffusion condition of temperature of 900 ºC for time of 3 h. Lower trace is the modulating voltage (1V/div), upper trace is the optical signal (5 V/div). The buffer layer was defined by 0.75 mm thickness of UV-15 polymer. (b) a photo of a waveguide device aligned with fibers.

4. Conclusion

A *Ni* in-diffused lithium niobate modulator with a polymer buffer layer was experimentally fabricated and characterized. By studying the mode size variations according to the diffusion time, the optimum fabrication condition was extracted. First, the mode size study suggested that the optical confinement at diffusion temperature of *900 ℃* for diffusion time of *1 h* was excellent, but the mode size in depth and width was not comparable to that of a standard single mode fiber. In order to determine diffusion parameters to simultaneously achieve good waveguide-fiber mode match and low propagation loss, the diffusion time was increased. As a result, the waveguide fabrication condition incorporating with diffusion time of *3 h* was selected to prepare the optical waveguides which offers more compatible mode size to that of fiber. The measured coupling loss of *~0.43dB* and propagation loss of *1.39 dB/cm* have been achieved. Second, a simple approach model for analyzing the polymer buffer layer effects on driving voltage was used. Finally, a *Ni* in-diffused lithium niobate modulator was developed with a polymer buffer layer using the fabrication parameters resulted from described above; the fabricated device shows a driving voltage of *9.89 V* and extinction ratio of over *17.5 dB* and the fiber to fiber insertion loss was found to be less than *7.12 dB*. Moreover, It is found that the fabrication process of the *Ni* in-diffused optical modulator can be significantly simplified by using the polymer buffer layer because of easy fabrication-process compared with that of silicon oxide buffer layer.

References

[1] R.V.Schmidt and I.P.Kaminow, Appl. Phys.Lett., 25, 8, 458 (1974).

[2] J.L.Jackel, C.E.Rice, and J.J.Veselka, Appl. Phys. Lett., 41, 7, 607 (1982).

[3] Yu-Pin Liao, Der-Jung Chen, Ruei-Chang Lu, and Way-Seen Wang, IEEE Photonics Technology Letters, 8, 4, 548 (1996).

[4] Wen-Ching Chang, Chao-Yung Sue. Hung-Ching Hou, and Ming-Yung Hsuan, Microwave and Optical Technology Letters, 22, 5, 358 (1999).

[5] P.K.Wei and W.S.Wang, Microwave Opt. Technol. Lett., 7, 5, 219 (1994).

[6] Ruey-Chang Twu, Chia-Chih Huang and Way-Seen Wang, Electron Lett., 36, 3, 220 (2000).

[7] M.N. Armenise, Proc. J. Inst. Elec. Eng. 22. 85 (1988).

[8] K.R.Suresh Nair, Y.G.K.Patro, and R.K. Shevgaonkar, Microwave and Optical Technology Letters, 19, 6, 448 (1998).
[9] Minchel Oh, Hua Zhang, Attila Szep, Vadim Chuyanov, William H. Steir, Cheng Zhang, Larry R. Dalton, Heman Erlig, Boris Tsap, and H. R. Fetterman, Applied Physics Letters, 76, 24, 3525 (2000).
[10] R.A.Becker and B.E.Kincaid, J of Lightwave Technology, 11, 12, 2076 (1993).
[11] C.M.Kim and R.V.Ramaswamy, J of Lightwave Te chnology, 7, 1063 (1989).
[12] K.Noguchi, T.Suzuki, M.Yanagibashi, H.Miyazawa, and O.Mitomi, NTT R&D, 41, 9, 1103 (1992).
[13] A.Neyer and T.Pohlmann, Electron Lett., 23, 22, 1187 (1987).
[14] Kwon-Wah Hui, Bo-Yu Wu, and K.S.Chiang, Microwave and Optical Technology Letters, 14, 5, 305 (1997).
[15] W.K.Burns and G.B.Hocker, Applied Optics, 16, 8, 2048 (1977).
[16] R.C.Alferness, V.R.Ramaswamy, S.K. Korotky, M.D.Divino, and L.L.Buhl, IEEE J.of Quantum Electronics, QE-18, 10, 1807 (1982).
[17] E.J.Murphy, T.C.Rice, L.Mccaughan, G.T. Harvey, and P.H.Read, J.of Lightwave Technology, LT-3, 4, 795 (1985).
[18] C.Sabarier, and E.Caquot, IEE J. of Quantum Electronics, QE-22, 1, 32 (1986).
[19] Technical Data Sheet which is offered by Master Bond polymer systems, 154 Hobert Street Hackensack, N.J. 07601-3922.
[20] L. Thylen, and Per Granestrand, J. Opt. Commun, 7, 1, 11 (1986).
[21] H.Chung, W.S.C.Chang, and E.L.Adler, IEEE J. of. Quantum Electronics, 27, 3, 608 (1991).